American Mineralogist, Volume 92, pages 662–669, 2007

Neptunium incorporation in sodium-substituted metaschoepite

Amanda L. Klingensmith,[1] Kathryn M. Deely,[1] William S. Kinman,[1] Virginia Kelly,[1] and Peter C. Burns[1,2,*]

[1]Department of Civil Engineering and Geological Sciences, University of Notre Dame, 156 Fitzpatrick Hall, Notre Dame, Indiana 46556, U.S.A.
[2]Chemistry Division, Argonne National Laboratory, Argonne, Illinois 60439, U.S.A.

Abstract

Uranyl oxide hydrate minerals are common in the altered zones of U deposits and are expected to form where spent nuclear fuel is altered in an oxidizing environment. Consistent with all known uranyl oxide hydrate minerals, metaschoepite $[(UO_2)_4O(OH)_6](H_2O)_5$, contains sheets of uranyl polyhedra with H_2O groups located in the interlayer. Several crystals along the series from metaschoepite to Na-substituted metaschoepite (Na-MS), approximate formula $Na[(UO_2)_4O_2(OH)_5](H_2O)_5$, have been synthesized and their structures have been determined. Each contains sheets of uranyl pentagonal bipyramids that are topologically identical to those in metaschoepite, schoepite and fourmarierite. The sheets are electroneutral in metaschoepite, but substitution of O for OH located at the equatorial vertices of the uranyl polyhedra gives a charged sheet that is balanced by incorporation of Na in the interlayer. Synthesis of crystals of Na-MS from a solution containing ~500 ppm Np^{5+}, followed by analysis of the crystals using laser-ablation inductively coupled-plasma mass-spectroscopy, demonstrated that the crystals incorporate Np. This is in contrast to earlier studies that showed no incorporation of Np^{5+} in synthetic metaschoepite (which has electroneutral sheets), and supports the hypothesis that Np^{5+} incorporation is more likely in uranyl oxide hydrates with charged species in the interlayer.

Keywords: Metaschoepite, uranyl, uranium, nuclear waste, geologic repository, crystal structure, neptunium

Introduction

Hexavalent U (uranyl) minerals occur in the oxidized zones of U deposits, where it is common for several uranyl mineral species to coexist, often in intimate intergrowths (Frondel 1958; Finch and Ewing 1992). Uranyl oxide hydrate minerals are typically the first to form during the onset of alteration of uraninite (Finch and Ewing 1992). Uranyl oxide hydrates have been the focus of considerable research recently, including analysis of their crystal structures (Burns 2005), the relationships between their structures and crystal morphology (Schindler et al. 2004a, 2004b, 2004c), and their thermodynamic properties (Kubatko et al. 2006). About 20 species have been described, and the structures are known for 16 of these (Burns 2005). In all cases the structures consist of sheets of uranyl polyhedra. The interlayer regions always contain H_2O in these minerals, and in all but schoepite and metaschoepite the interlayers also contain lower-valence cations (Burns 2005).

The crystal structures of schoepite, $[(UO_2)_8O_2(OH)_{12}](H_2O)_{12}$ (Finch et al. 1996), metaschoepite, $[(UO_2)_4O(OH)_6](H_2O)_5$ (Weller et al. 2000) and fourmarierite, $Pb[(UO_2)_4O_3(OH)_4](H_2O)_4$ (Piret 1985) contain topologically identical sheets formed by the sharing of edges and vertices between uranyl pentagonal bipyramids. In each structure, the uranyl ions are oriented roughly perpendicular to the plane of the sheet, and linkages between the polyhedra are through equatorial edges and vertices only. In the case of fourmarierite, the sheet of uranyl polyhedra has a net negative charge and Pb^{2+} cations are located in the interlayer. The structures of metaschoepite and schoepite contain chemically identical sheets that are electroneutral, and the sheets are linked through H bonds extending to and from H_2O groups located in the interlayers of the structures.

Alteration of spent nuclear fuel in a geological repository contained within the unsaturated zone, such as the proposed geological repository at Yucca Mountain, Nevada, is likely to result in a suite of uranyl phases that will include uranyl oxide hydrates. Wronkiewicz et al. (1992, 1996) examined the alteration of unirradiated UO_2 in slowly dripping water at 90 °C over ten years. The water used was from well J-13 at the Yucca Mountain site, and was reacted with crushed Tonopah Springs tuff at 90 °C for 80 days. The resulting water, designated EJ-13, contains more Na and Si than J-13 water, with Na and Si concentrations of 46.5 and 34.4 µg/mL, respectively (Wronkiewicz et al. 1992). Alteration of the UO_2 in these studies was rapid, and resulted in a suite of uranyl oxide hydrate and uranyl silicate minerals, with the uranyl oxide hydrates being the first to form at the onset of alteration. Metaschoepite was observed to form early following the onset of alteration (Wronkiewicz et al. 1996). In similar studies using commercial spent nuclear fuel and EJ-13 water, Finch et al. (1999) also reported the formation of metaschoepite when water was dripped onto the spent fuel, and also when the spent fuel altered in the absence of dripping water, but in an atmosphere with 100% relative humidity.

Burns et al. (1997a) proposed that uranyl minerals that form

* E-mail: pburns@nd.edu

0003-004X/07/0004–662$05.00/DOI: 10.2138/am.2007.2350

due to the alteration of spent nuclear fuel in a geological repository may incorporate various radionuclides, thereby reducing their mobility in the repository environment. Owing to its long half-life (2.14 million years) and potential solubility in groundwater, Np may be a significant dose contributor during the long-term storage of nuclear waste in an unsaturated-zone repository. Burns et al. (2004) synthesized uranyl minerals in the presence of 10 to 400 ppm Np^{5+}, and analyzed the resulting fine-grained powders. Significant Np was found in association with powders of uranophane and the Na analog of compreignacite, but Np was not found associated with synthetic metaschoepite that formed under similar conditions. Skanthakumar et al. (2004) used X-ray absorption near edge spectra (XANES) to demonstrate that the Np contained in powders of the Na analog of compreignacite was dominantly in the pentavalent state. This result is significant because Np^{5+} is soluble in groundwater, whereas the solubility of Np^{4+} is much lower.

In the course of several studies of the interaction of uranyl-bearing solutions with geologic materials, we have obtained well-formed crystals of a new phase that is chemically and structurally closely related to metaschoepite. This phase, hereafter designated Na-MS, contains essential Na, but most of its properties, including its X-ray powder diffraction pattern and unit-cell dimensions, are virtually indistinguishable from those of metaschoepite. In addition to studying the structure of several crystals of Na-MS, we refined the structure of a natural crystal of metaschoepite for comparison to the structure provided for a synthetic analog by Weller et al. (2000). Burns and Klingensmith (2006) first reported formation of Na-MS and incorporation of Np into its crystal structure. Here we provide details of the syntheses and structures of multiple crystals, and expand the discussion of it structure and incorporation of Np.

Experimental methods

Crystal syntheses

Crystals of Na-MS obtained in four different synthesis experiments were selected for study by X-ray diffraction. Crystals (designated Na-MS-CRY) were synthesized by reacting 4 mL of a 0.2 *M* uranyl acetate solution with 0.3 g of crystal fragments of natural cryolite. The solution pH was adjusted to 4 by addition of dilute HCl. The solution and cryolite were placed in a 23 mL Teflon-lined reaction vessel that was sealed and heated at 120 °C for 7 days. Slow dissolution of the cryolite crystals provided for nucleation and growth of tabular crystals of Na-MS that reached 200 μm in maximum dimension. To examine the possible incorporation of trace levels of Np^{5+} into the structure of Na-MS, the synthesis using cryolite was repeated with the solution spiked with ~500 ppm Np^{5+} (designated Na-MS-CRY-Np). In this experiment, the reactants were contained in a 7 mL Teflon cup with a screw-top cap that was placed in a 120 mL Teflon-lined reaction vessel. Fifty mL of ultrapure water was added to the vessel to provide counter-pressure during heating.

During the course of studying the interaction of uranyl bearing solutions with crystals of natural albite, crystals of Na-MS formed. The crystals of Na-MS appeared on crystals of albite that had been soaked in a 0.001 *M* solution of uranyl acetate (designated Na-MS-AB1) and in a 0.01 *M* solution of uranyl acetate (designated Na-MS-AB2) sealed in 23 mL Teflon-lined reaction vessels at 80 °C for two weeks. Formation of the Na-MS crystals was promoted by the slow dissolution of albite, which released Na into solution.

Natural specimen

A crystal of natural metaschoepite was acquired from the Harvard museum. The specimen was uncatalogued and is labeled "Paraschoepite – Schoep type material, Katanga, Congo." No further information is known concerning the history of the specimen. Paraschoepite was defined by Schoep and Stradiot (1947) with the formula $5UO_3 \cdot 9½H_2O$. Christ and Clark (1960) reported paraschoepite from a sample that also contained schoepite. Metaschoepite was also described by Christ and Clark (1960) with the formula $UO_3 \cdot 2H_2O$. Considerable progress has been made in understanding the structures and chemistry of both schoepite (Finch et al. 1996) and metaschoepite (Weller et al. 2000), and both have been synthesized. The unit-cell dimensions obtained for the natural crystal studied here (Table 1) are consistent with metaschoepite but not with those of paraschoepite provided by Christ and Clark (1960). Further details concerning the distinction of the various schoepite-like minerals are provided by Finch et al. (1998).

X-ray data collection

Single-crystal X-ray diffraction data were collected for each of the four synthetic materials and for a natural crystal of metaschoepite using a Bruker three-circle diffractometer equipped with an APEX CCD detector, graphite-monochromatized Mo$K\alpha$ radiation, and a crystal-to-detector distance of 4.67 cm. A sphere of three-dimensional data was collected for each crystal except Na-MS-AB2, for which more than a hemisphere of data was collected. The diffraction data were collected using frame widths of 0.3° in ω and from 20 to 30 s spent counting per frame. Unit-cell dimensions were refined by least-squares techniques using the positions of reflections selected from the data. Intensity data were corrected for Lorentz, polarization and background effects using the Bruker program SAINT. Data were corrected for absorption semi-empirically by modeling the crystals as plates; reflections having a plate-glancing angle less than 3° were discarded. Crystallographic details for each crystal are provided in Table 1.

Chemical analyses

Samples were first examined using an LEO EVO-50XVP variable pressure/high humidity scanning electron microscope. An SEM image of crystals of Na-MS-AB2 is provided in Figure 1. Energy dispersive spectroscopy verified the presence of U and Na in the crystals, and also revealed the presence of F in crystals synthesized in the presence of cryolite.

Selected crystals were subsequently mounted, polished, and coated with C for analyses using a JEOL 8600 electron microprobe. Standards used were synthetic UO_2, synthetic CaF_2, and Amelia albite. Two grains were analyzed for each material. The UO_3 concentrations obtained from the microprobe were consistently higher than expected (ranging from 90.4 to 95.6 wt%), indicating loss of volatiles that presumably include H_2O and Na that are located in the interlayers of the structure. It is possible that the volatiles were quickly lost in the vacuum of the instrument, during sample preparation, or during irradiation with the electron beam. The analyses for Na are not considered reliable, but they did confirm the presence of Na in each crystal. Furthermore, an X-ray photoelectron spectrum (XPS) provided by M. Schindler for our synthetic crystals confirmed the presence of Na. In the case of Na-MS-CRY the analyses also indicated from 1.4 to 2.0 wt% F in the crystals (Na-MS-CRY-Np was not analyzed using the electron microprobe).

As discussed by Burns and Klingensmith (2006), determination of the Np concentration in Na-MS-CRY-Np presents a significant challenge, as spatial resolution and high sensitivity is needed for the examination of the single crystals.

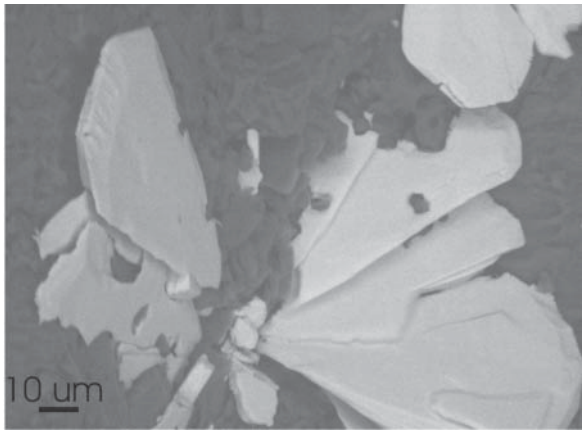

Figure 1. SEM image of crystals of Na-MS-AB2 that grew on the surface of albite during hydrothermal treatment.

Table 1. Crystallographic and refinement information for crystals of Na-MS

	Natural	Na-MS-CRY	Na-MS-CRY-Np	Na-MS-AB1	Na-MS-AB2	Weller et al. (2000)
a (Å)	14.6801(16)	14.7050(6)	14.6401(15)	14.6317(27)	14.6592(9)	14.6861(4)
b (Å)	14.0287(15)	14.0565(5)	14.0417(14)	14.0147(25)	14.0358(8)	13.9799(3)
c (Å)	16.7196(17)	16.7051(6)	16.7044(17)	16.6977(30)	16.7148(10)	16.7063(5)
V (Å^3)	3443.28	3452.96	3433.96	3424.01	3439.13	3429.97
Space group	*Pbcn*	*Pbcn*	*Pbcn*	*Pbcn*	*Pbcn*	*Pbcn*
$2\theta_{max}$(°)	69.2	69.1	69.1	69.4	69.0	
Total reflections	59442	64326	61804	63926	32006	
Unique reflections	7190	7295	7247	7249	7059	
Data with $F > 4\sigma(F)$	3399	4349	2482	2908	3718	
*R*1 (%)	5.49	3.45	5.28	6.24	3.92	
*wR*2 (%)	10.34	6.15	7.83	12.15	6.97	
S	1.13	0.93	0.73	0.84	0.77	
Parameters	124	194	164	194	194	

$R1 = \Sigma(|F_o| - |F_c|)/\Sigma|F_o| \times 100$; $wR2\ [\Sigma w(F_o^2 - F_c^2)^2/\Sigma w(F_o^2)^2]^{1/2}$; $S = [\Sigma w(|F_o| - |F_c|)^2/(m-n)]^{1/2}$
$w = 1/[\sigma^2(F_o^2) + (0.0314 \times P)^2]$, $P = (\max(F_o^2,0) + 2 \times F_c^2)/3$

The analysis is further complicated by the need to quantify a few parts per million of Np in a sample containing tens of weight percent U. A New Wave UP 213 nm laser was used to ablate single crystals directly into a high-resolution magnetic sector ELEMENT 2 inductively coupled plasma mass spectrometer for the analysis of Np. Prior to analyzing the Np-bearing crystal, crystals grown in the absence of Np (Na-MS-CRY) were analyzed to verify that there is no interference of the 238 mass isotope of U with the 237 mass window selected for the analysis. The results for a crystal of Na-MS-CRY-Np are shown in Figure 2, taken from Burns and Klingensmith (2006).

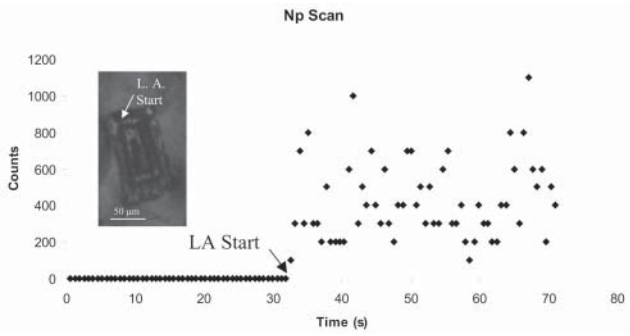

Figure 2. Laser-ablation ICP-MS data for Np-237 from a crystal of Na-substituted metaschoepite synthesized from a solution containing approximately 500 ppm Np^{5+}. The crystal analyzed is shown as an inset, where the ablation track is apparent. From Burns and Klingensmith (2006).

Structure refinements

On the basis of the similarity of the unit cells of Na-MS-CRY and synthetic metaschoepite, refinement of the structure was commenced using space group *Pbcn* and the atomic coordinates for synthetic metaschoepite from Weller et al. (2000) as the starting model. Inspection of the preliminary model revealed that the OW20 and OW21 sites of metaschoepite, which are occupied by H_2O located in the interlayer, were absent in Na-MS-CRY. However, the locations of the U atoms and O atoms from O1 to OW19 of metaschoepite had equivalent sites in Na-MS-CRY. Inspection of difference-Fourier maps calculated for the partial-structure model revealed four additional sites in the interlayer region. Each of these sites exhibits some degree of positional disorder and partial occupancy, as evidenced by relatively large refined displacement parameters. The final structure model, which was refined on the basis of F^2 for all unique reflections, included all atomic positional parameters, anisotropic displacement parameters for the U sites and O sites number from O1 to OH14, an isotropic displacement parameter for the OH15 site, and fixed isotropic displacement parameters and refined occupancy factors for O sites numbered OW16 through OW22. The OW16 atom is distributed over two closely spaced sites designated OW16a and OW16b. The OW21 site is displaced off the special position, such that symmetrically equivalent OW21 sites are separated by ~0.8 Å, and only one can be occupied locally. Crystallographic parameters and refinement statistics are presented in Table 1 and atomic positional parameters and site occupancy factors are in Table 2, and additional displacement structural parameters are in Table 3.[1]

The structures of natural metaschoepite, Na-MS-AB1, Na-MS-AB2, and Na-MS-CRY-Np were refined using the structure of Na-MS-CRY as the starting model. Data quality varied for these crystals, and in some cases the data did not support refinement of anisotropic displacement parameters for the O sites. Otherwise, the refinement strategy for these crystals was the same as for Na-MS-CRY, and the occupancies of the OW16 through OW22 sites were refined with their corresponding displacement parameters fixed. Crystallographic parameters for each are given in Table 1. Atomic parameters are in Table 2. Selected interatomic distances for the five refined structures, as well as those of Weller et al. (2000) for synthetic metaschoepite, are compared in Table 4.

Structure description

The structures of each crystal under study contain four symmetrically distinct U^{6+} cations, and each are strongly bonded to two atoms of O, resulting in approximately linear $(UO_2)^{2+}$ uranyl ions. The uranyl ions are each coordinated by a total of five O atoms and hydroxyl groups, and these ligands are arranged at the equatorial vertices of pentagonal bipyramids that are capped by the O atoms of the uranyl ions (Table 4).

The uranyl pentagonal bipyramids are linked by sharing equatorial edges, which results in sheets that are topologically

Deposit item Am-07-017, Table 3 in CIF format. Deposit items are available two ways: For a paper copy contact the Business Office of the Mineralogical Society of America (see inside front cover of recent issue) for price information. For an electronic copy visit the MSA web site at http://www.minsocam.org, go to the American Mineralogist Contents, find the table of contents for the specific volume/issue wanted, and then click on the deposit link there.

TABLE 2. Atomic coordinated and equivalent isotropic displacement parameters for crystals of Na-MS

Natural		MS	Na-MS-CRY	Na-MS-CRY-Np	Na-MS-AB1	Na-MS-AB2	Weller et al. 2000
U(1)	x	0.23381(4)	0.23566(2)	0.23574(4)	0.23479(4)	0.23414(3)	0.23453(4)
	y	0.74397(3)	0.73997(2)	0.74017(4)	0.74265(4)	0.74380(2)	0.74724(4)
	z	0.37478(3)	0.38244(1)	0.38168(3)	0.37739(3)	0.37476(2)	0.36301(4)
	U(eq)	0.01545(12)	0.01284(6)	0.01471(3)	0.01824(5)	0.01425(8)	0.01561(18)
U(2)	x	0.28634(4)	0.27743(2)	0.27735(4)	0.28370(5)	0.28636(3)	0.29656(5)
	y	0.76845(3)	0.76403(2)	0.76422(4)	0.76835(4)	0.76851(2)	0.77012(4)
	z	0.60325(3)	0.61003(2)	0.60929(3)	0.60448(3)	0.60317(2)	0.59321(4)
	U(eq)	0.01605(12)	0.01368(6)	0.01475(3)	0.01861(4)	0.01568(8)	0.01655(19)
U(3)	x	0.25577(5)	0.25494(2)	0.25531(5)	0.25685(5)	0.25637(3)	0.25426(5)
	y	0.51214(3)	0.51522(2)	0.51527(4)	0.51221(4)	0.51220(3)	0.51155(4)
	z	0.23933(3)	0.24274(1)	0.24250(3)	0.24135(3)	0.23921(2)	0.22973(4)
	U(eq)	0.01607(13)	0.01410(7)	0.01534(4)	0.01698(5)	0.01576(9)	0.01706(19)
U(4)	x	0.25591(5)	0.25380(3)	0.25387(6)	0.25692(6)	0.25652(3)	0.25432(5)
	y	0.51731(3)	0.51705(2)	0.51696(4)	0.51835(4)	0.51717(2)	0.51460(4)
	z	0.51083(3)	0.51584(1)	0.51512(3)	0.51248(4)	0.51109(2)	0.50131(4)
	U(eq)	0.01707(12)	0. 01329(6)	0.01435(3)	0. 02173(6)	0.01603(9)	0.01630(19)
O(1)	x	0.1748(8)	0.1613(5)	0.1684(7)	0.170(1)	0.1683(5)	0.1802(9)
	y	0.7406(6)	0.7403(4)	0.7423(7)	0.7462(8)	0.7458(4)	0.7479(7)
	z	0.6145(6)	0.6273(4)	0.6263(7)	0.6131(8)	0.6126(5)	0.5935(8)
	U(eq)	0.035(3)	0.032(1)	0.030(3)	0.042(4)	0.032(2)	0.032(3)
O(2)	x	0.1475(8)	0.1407(5)	0.1449(9)	0.151(1)	0.1452(6)	0.1438(8)
	y	0.4622(7)	0.4769(4)	0.4774(9)	0.4654(8)	0.4616(5)	0.4529(7)
	z	0.2320(6)	0.2292(3)	0.2305(6)	0.2326(7)	0.2319(4)	0.2244(7)
	U(eq)	0.032(3)	0.031(2)	0.032(3)	0.037(4)	0.029(2)	0.028(3)
O(3)	x	0.1206(7)	0.1205(4)	0.1203(7)	0.1206(8)	0.1225(5)	0.1293(8)
	y	0.7443(6)	0.7514(3)	0.7522(8)	0.7424(8)	0.7450(4)	0.7449(7)
	z	0.4156(6)	0.4139(3)	0.4109(6)	0.4156(6)	0.4163(4)	0.4127(7)
	U(eq)	0.026(2)	0.025(1)	0.029(3)	0.024(3)	0.020(2)	0.026(3)
O(4)	x	0.4098(7)	0.3964(4)	0.3960(7)	0.4025(8)	0.4057(5)	0.4167(7)
	y	0.7847(6)	0.7804(3)	0.7779(9)	0.7837(7)	0.7845(4)	0.7849(7)
	z	0.5968(5)	0.6015(3)	0.6012(6)	0.5983(6)	0.5964(4)	0.5914(7)
	U(eq)	0.019(2)	0.018(1)	0.029(3)	0.021(3)	0.019(2)	0.022(3)
O(5)	x	0.3678(7)	0.3692(4)	0.3693(7)	0.3715(8)	0.3699(5)	0.3642(8)
	y	0.5610(7)	0.5517(4)	0.5483(8)	0.5586(9)	0.5601(5)	0.5633(7)
	z	0.2511(6)	0.2597(3)	0.2620(7)	0.2508(7)	0.2511(4)	0.2359(7)
	U(eq)	0.024(2)	0.025(1)	0.024(3)	0.027(3)	0.023(2)	0.026(3)
O(6)	x	0.1391(7)	0.1372(4)	0.1368(8)	0.1415(9)	0.1407(6)	0.1416(7)
	y	0.5483(6)	0.5388(4)	0.5341(8)	0.5477(9)	0.5489(5)	0.5579(7)
	z	0.5295(6)	0.5383(3)	0.5368(7)	0.5317(8)	0.5293(4)	0.5179(7)
	U(eq)	0.021(2)	0.021(1)	0.021(3)	0.035(4)	0.027(2)	0.023(3)
O(7)	x	0.3420(8)	0.3487(4)	0.3473(6)	0.3449(8)	0.3449(5)	0.3385(8)
	y	0.7440(6)	0.7302(4)	0.7328(8)	0.7419(8)	0.7463(5)	0.7524(7)
	z	0.3315(6)	0.3469(3)	0.3479(6)	0.3368(7)	0.3310(4)	0.3101(8)
	U(eq)	0.028(2)	0.026(1)	0.019(2)	0.024(3)	0.026(2)	0.034(3)
O(8)	x	0.3699(8)	0.3694(5)	0.3666(9)	0.367(1)	0.3721(6)	0.3692(8)
	y	0.4841(7)	0.4935(4)	0.4960(9)	0.4875(9)	0.4840(5)	0.4724(7)
	z	0.4895(6)	0.4889(4)	0.4876(7)	0.4898(7)	0.4895(4)	0.4845(7)
	U(eq)	0.027(2)	0.029(2)	0.028(3)	0.049(5)	0.029(2)	0.025(3)
O(9)	x	0.2517(7)	0.2419(4)	0.2417(7)	0.249(1)	0.2524(6)	0.2652(7)
	y	0.9229(6)	0.9185(3)	0.9217(6)	0.9237(8)	0.9225(4)	0.9236(7)
	z	0.6173(5)	0.6219(3)	0.6212(5)	0.6195(6)	0.6175(4)	0.4591(7)
	U(eq)	0.018(2)	0.022(1)	0.012(2)	0.033(3)	0.029(2)	0.019(3)
OH(10)	x	0.2082(7)	0.2113(4)	0.2137(7)	0.2085(9)	0.2053(6)	0.2028(8)
	y	0.3619(6)	0.3613(3)	0.3604(7)	0.3638(7)	0.3617(4)	0.3615(6)
	z	0.4680(5)	0.4716(3)	0.4705(5)	0.4705(6)	0.4686(4)	0.4591(7)
	U(eq)	0.020(2)	0.017(1)	0.013(2)	0.023(3)	0.019(2)	0.019(3)
O(11)	x	0.2928(8)	0.2737(4)	0.2730(7)	0.290(1)	0.2966(7)	0.3125(7)
	y	0.6751(6)	0.6741(3)	0.6734(7)	0.6729(8)	0.6736(5)	0.6719(6)
	z	0.4885(6)	0.4984(2)	0.4989(6)	0.4909(7)	0.4881(4)	0.4737(6)
	U(eq)	0.028(2)	0.025(3)	0.018(2)	0.042(4)	0.040(3)	0.016(3)
OH(12)	x	0.2144(6)	0.2116(4)	0.2141(7)	0.2147(8)	0.2123(5)	0.2152(7)
	y	0.5628(5)	0.5622(3)	0.5627(7)	0.5635(7)	0.5634(4)	0.5667(7)
	z	0.3722(5)	0.3782(3)	0.3764(6)	0.3747(6)	0.3726(3)	0.3635(7)
	U(eq)	0.014(2)	0.015(1)	0.016(2)	0.021(3)	0.018(2)	0.021(3)

*Occupancies were refined using the atomic scattering factors for O. Na substitutes at various OW sites.

Continued on next page

identical to those found in the structures of metaschoepite, schoepite, and fourmarierite (Fig. 3). However, examination of the bond-strength distributions within the uranyl polyhedra reveals that the composition of the sheets in the structures under study are not the same as that of the electroneutral sheets in metaschoepite and schoepite.

Consider the structure of metaschoepite (Weller et al. 2000). Atoms O1 through O8 are part of uranyl ions. Atoms O9 through OH15 are all at equatorial vertices of the uranyl pentagonal bipyramids, and O9 through OH14 are each bonded to three U^{6+} cations, whereas OH15 is bonded to two. The bond valences, calculated using the parameters of Burns et al. (1997b), incident upon the OH10 through OH15 sites due to the bonds to U^{6+} range from 1.19 to 1.44 v.u., all of which are consistent with occupancy

TABLE 2. —*Continued*

Natural		MS	Na-MS-CRY	Na-MS-CRY-Np	Na-MS-AB1	Na-MS-AB2	Weller et al. 2000
OH(13)	x	0.3117(7)	0.3086(4)	0.3058(7)	0.3121(8)	0.3123(5)	0.3121(7)
	y	0.6015(6)	0.6001(3)	0.6004(7)	0.6030(7)	0.6005(4)	0.6007(7)
	z	0.6385(5)	0.6456(3)	0.6460(5)	0.6412(6)	0.6387(4)	0.6270(6)
	U(eq)	0.017(2)	0.015(1)	0.013(2)	0.020(3)	0.017(2)	0.019(3)
OH(14)	x	0.1883(7)	0.1936(4)	0.1921(6)	0.1893(7)	0.1869(5)	0.1846(7)
	y	0.6854(6)	0.6859(3)	0.6845(7)	0.6840(7)	0.6830(4)	0.6852(7)
	z	0.2439(5)	0.2487(3)	0.2491(6)	0.2449(6)	0.2435(4)	0.2342(7)
	U(eq)	0.015(2)	0.015(1)	0.017(2)	0.018(2)	0.017(2)	0.022(3)
OH(15)	x	0.1894(7)	0.2137(4)	0.2108(7)	0.1907(8)	0.1880(5)	0.1863(7)
	y	0.8851(6)	0.8797(3)	0.8793(7)	0.8841(8)	0.8848(4)	0.8888(6)
	z	0.3128(5)	0.3137(3)	0.3133(6)	0.3156(7)	0.3135(4)	0.3066(6)
	U(eq)	0.016(2)	0.013(1)	0.015(2)	0.022(3)	0.018(2)	0.018(3)
OW(16A)	x	0	0	0	0	0	0
	y	0.753(2)	0.723(3)	0.738(6)	0.755(5)	0.751(2)	0.7609(12)
	z	0.25	0.25	0.25	0.25	0.25	0.25
	U(eq)	0.04	0.04	0.04	0.04	0.04	0.049(5)
	Occ*	60(2)	40(2)	32(3)	23(2)	38(1)	
OW(16B)	x	0	0	0	0	0	
	y	0.659(2)	0.681(3)	0.683(3)	0.662(2)	0.654(2)	
	z	0.25	0.25	0.25	0.25	0.25	
	U(eq)	0.04	0.04	0.04	0.04	0.04	
	Occ*	48(2)	46(2)	60(3)	74(2)	48(1)	
OW(17)	x	0.499(1)	0.4924(6)	0.495(1)	0.501(1)	0.5004(9)	0.5015(9)
	y	0.418(1)	0.4026(5)	0.4039(9)	0.405(1)	0.4164(9)	0.4409(9)
	z	0.1442(9)	0.1551(5)	0.1489(7)	0.145(1)	0.1427(7)	0.1386(9)
	U(eq)	0.04	0.04	0.04	0.04	0.04	0.048(4)
	Occ*	78(2)	78(1)	98(2)	75(3)	68(2)	
OW(18)	x	–0.0196(9)	–0.0195(5)	–0.0163(9)	–0.018(1)	-0.0234(8)	–0.0253(10)
	y	0.6443(8)	0.6642(5)	0.6641(9)	0.6485(1)	0.6449(7)	0.6223(10)
	z	0.5691(8)	0.5530(4)	0.5496(7)	0.5637(9)	0.5705(6)	0.5870(10)
	U(eq)	0.04	0.04	0.04	0.04	0.04	0.060(4)
	Occ*	94(2)	97(1)	100(2)	87(3)	80(2)	
OW(19)	x	0.027(1)	0.0272(5)	0.0233(8)	0.026(1)	0.0294(8)	0.0314(9)
	y	0.549(1)	0.5486(5)	0.5480(9)	0.545(1)	0.5496(7)	0.5621(8)
	z	0.3679(8)	0.3775(4)	0.3758(7)	0.3768(9)	0.3701(6)	0.3391(8)
	U(eq)	0.04	0.04	0.04	0.04	0.04	0.046(4)
	Occ*	81(2)	93(1)	99(3)	89(3)	78(2)	
OW(20)	x	0.497(1)	0.5067(7)	0.506(1)	0.498(2)	0.496(1)	–0.119(11)
	y	0.647(1)	0.6224(6)	0.621(1)	0.637(2)	0.6404(9)	0.8529(11)
	z	0.422(1)	0.4010(6)	0.402(1)	0.415(1)	0.4199(8)	0.5792(10)
	U(eq)	0.04	0.04	0.04	0.04	0.04	0.081(5)
	Occ*	63(2)	67(1)	70(2)	61(3)	60(2)	
OW(21)	x	0.503(3)	0.502(1)	0.501(2)	0.506(2)	0.510(3)	0.517(3)
	y	0.672(3)	0.6593(7)	0.663(1)	0.676(2)	0.684(2)	0.758(2)
	z	0.295(2)	0.2756(6)	0.284(1)	0.283(1)	0.276(2)	0.287(2)
	U(eq)	0.04	0.04	0.04	0.04	0.04	0.096(13)
	Occ*	24(2)	55(1)	61(2)	58(2)	24(1)	
OW(22)	x	0.5	0.5	0.5	0.5	0.5	0.5
	y	0.794(2)	0.8186(8)	0.820(2)	0.817(2)	0.809(2)	
	z	0.25	0.25	0.25	0.25	0.25	
	U(eq)	0.04	0.04	0.04	0.04	0.04	
	Occ*	52(2)	77.4(8)	84(2)	66(2)	50(1)	

* Occupancies were refined using the atomic scattering factors for O. Na substitutes at various OW sites.

of these sites by OH groups. The bond-valence sum at the O9 site, which forms substantially shorter bonds with U^{6+}, is 2.12 v.u., indicating that the site must be occupied by O. Compare to these values those from the structure of Na-MS-CRY. The O9 and O11 sites both have incident bond-valences of 2.05 v.u., which indicates both contain O only, in contrast to metaschoepite, for which the O11 site contains OH. The remaining sites in the range OH10 to OH15 in Na-MS-CRY have incident bond-valences in the range of 1.23 to 1.30 v.u., which indicates that each of these sites is occupied mostly by hydroxyl groups. The chemical analysis for crystals of Na-MS-CRY indicated they contain as much as 2 wt% F, which is presumably distributed over the OH sites.

The sheet of uranyl polyhedra in the structure of Na-MS-CRY has the approximate composition $[(UO_2)_4O_2(OH,F)_5]$, which has a net charge of –1. In metaschoepite and schoepite, the sheet composition is $[(UO_2)_4O(OH)_6]$, which is electroneutral, whereas the topologically identical sheet in fourmarierite has composition $[(UO_2)_4O_3(OH)_4]$, with a net charge of –2. The composition of the sheet of polyhedra in Na-MS-CRY is intermediate between those of metaschoepite and fourmarierite. The sheet anion-topologies (Burns et al. 1996) corresponding to the sheets in Na-MS-CRY, metaschoepite and fourmarierite are shown in Figure 4. Each vertex in the anion topology represents either an O atom or an OH group, and the locations of the OH groups are shown by circles.

The residual charge of the sheet in Na-MS-CRY is balanced by Na located in the interlayer. It is possible that any of the interlayer H_2O sites OW16 through OW22 contain some Na. The OW21 site appears to be most compatible with Na, as it is coordinated by six ligands at distances between 2.16 and 2.99 Å. Three of these are O atoms of uranyl ions located within the

sheets on either side, and three are H_2O groups that are located in the interlayer. The idealized formula for Na-MS-CRY is $Na[(UO_2)_4O_2(OH)_5](H_2O)_5$, neglecting the F that substitutes at OH sites.

The structures of each of the crystals Na-MS-CRY-Np, Na-MS-AB1, Na-MS-AB2 and natural metaschoepite appear to be intermediate between those of Na-MS-CRY and the structure of synthetic metaschoepite published by Weller et al. (2000). This is most apparent when the bonding environment about the O11 site is considered. In all of the structures it is bonded to three U^{6+} cations. In the structure of Weller et al. (2000), the <O11-U^{6+}> bond length is 2.42 Å, whereas it is 2.24 Å in Na-MS-CRY. In the other structures, it is 2.24, 2.28, 2.31, and 2.32 for Na-MS-CRY-Np, Na-MS-AB1, natural metaschoepite, and Na-MS-AB2, respectively. The refined occupancies of the OW16 through OW22 sites also vary amongst these structures, with the highest corresponding to Na-MS-CRY and Na-MS-CRY-Np and the lowest to Na-MS-AB2.

The unit-cell dimensions of the crystals studied, as well as those of synthetic metaschoepite studied by Weller et al. (2000), show significant variations. The situation in these structures is complex, with variations in the amount of OH at the O11 site, partial occupancies of the H_2O sites in the interlayer and the associated variability of their H bonding networks, and the substitution of Na for H_2O in the interlayer. Despite this, there is a linear relationship between the bond-valence sum incident upon the O11 site and the *b* unit-cell dimension (Fig. 5). The bond-valence sum at the site reflects the quantity of OH at the site. The higher the OH content of the O11 site, the larger the average O11-U^{6+} bond length, and the lower the bond-valence sum incident upon the O11 site. As OH enters the O11 site, the *b* repeat distance steadily decreases. If the size of the O11 site was the only factor, one would expect the opposite to occur. Thus, the decrease of the *b* dimension is presumably related to distortions of the sheet of uranyl polyhedra that facilitate enhanced H bonding from the O11 site to an interlayer H_2O group. Stronger H bonding might tend to pull the O11 atom further out of the plane of the U^{6+} cations (toward the interlayer), perhaps increasing the corrugation of the sheet, which would tend to decrease the *b* cell dimension.

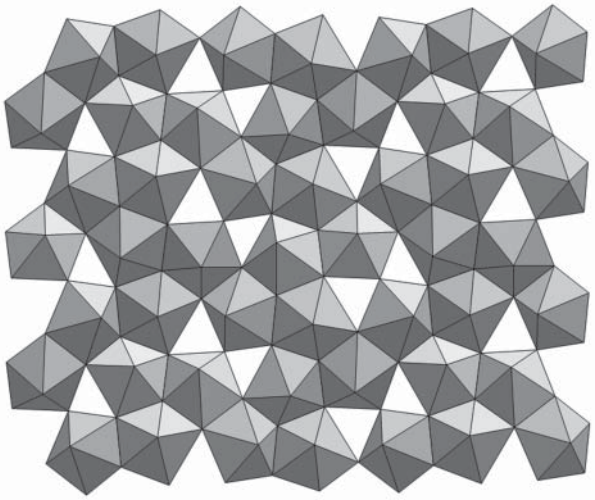

FIGURE 3. The sheet of uranyl pentagonal bipyramids that occurs in the structures of Na-MS as well as metaschoepite, fourmarierite and schoepite.

SUBSTITUTION OF NP INTO NA-MS-CRY-NP

The interaction of groundwater with spent nuclear fuel in a geological repository within the unsaturated zone, such as the proposed repository at Yucca Mountain, would likely entail the formation of a suite of uranyl minerals (e.g., Wronkiewicz et al. 1992, 1996, Finn et al. 1996, Finch et al. 1999). At the onset of alteration, temperatures may still be significantly elevated above ambient conditions. Simulations using spent nuclear fuel in contact with small amounts of water EJ-13 from the Yucca Mountain site resulted in the formation of a phase identified as metaschoepite (Finch et al. 1999). Given the relatively high abundance of Na in EJ-13 water (Na concentration of 54.1 ppm, Wronkiewicz et al. 1996), as well as in the groundwater associated with Yucca Mountain, it is possible that Na-MS formed in some of the simulations, and that it might be an important phase in the repository environment.

Burns et al. (2004) examined incorporation of Np^{5+} in powders of uranyl compounds synthesized under mild hydrothermal conditions. They found no significant incorporation in crystals of synthetic metaschoepite that were produced by reacting UO_3 with ultrapure water. However, Burns et al. (2004) did find that

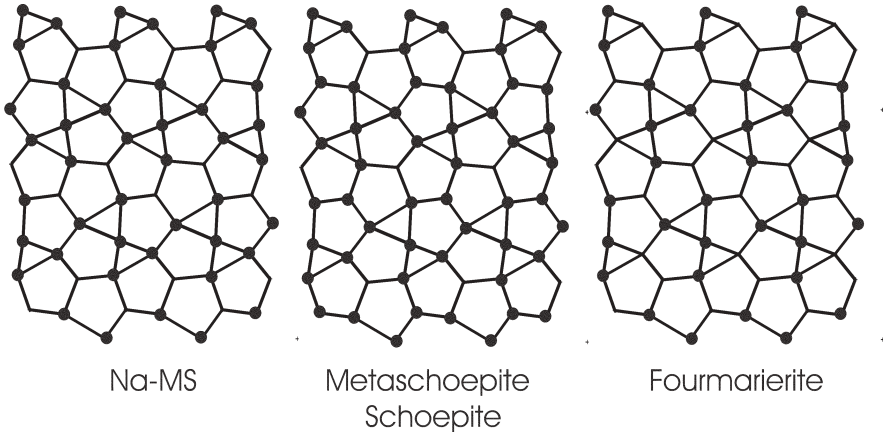

FIGURE 4. The sheet anion-topology that corresponds to the sheets in Na-MS-CRY, metaschoepite, and fourmarierite with the locations of OH groups indicated by circles. Vertices in the anion topology that do not contain OH correspond to O atoms.

TABLE 4. Selected interatomic distances for crystals of Na-MS

	Natural	Na-MS-CRY	Na-MS-CRY-Np	Na-MS-AB1	Na-MS-AB2	Weller et al. (2000)
U1–O7	1.745 (10)	1.770 (5)	1.731 (9)	1.747 (11)	1.781 (7)	1.766 (13)
U1–O3	1.796 (10)	1.780 (5)	1.767 (10)	1.788 (10)	1.777 (6)	1.754 (12)
U1–O11	2.302 (9)	2.219 (4)	2.238 (9)	2.281 (12)	2.323 (6)	2.416 (10)
U1–OH15	2.328 (8)	2.298 (4)	2.291 (10)	2.325 (11)	2.327 (6)	2.303 (9)
U1–OH10	2.426 (8)	2.395 (4)	2.366 (9)	2.447 (10)	2.445 (6)	2.445 (10)
U1–OH14	2.430 (8)	2.439 (4)	2.433 (10)	2.452 (10)	2.453 (6)	2.433 (11)
U1–OH12	2.558 (7)	2.524 (4)	2.513 (9)	2.527 (9)	2.552 (5)	2.540 (9)
U2–O1	1.693 (11)	1.764 (6)	1.648 (11)	1.698 (14)	1.767 (7)	1.737 (13)
U2–O4	1.829 (9)	1.769 (5)	1.753 (11)	1.754 (11)	1.767 (7)	1.777 (11)
U2–O9	2.327 (7)	2.242 (4)	2.280 (9)	2.249 (11)	2.230 (6)	2.208 (9)
U2–O11	2.325 (9)	2.253 (4)	2.242 (8)	2.323 (12)	2.344 (6)	2.434 (10)
U2–OH13	2.443 (7)	2.423 (4)	2.417 (9)	2.432 (9)	2.461 (5)	2.446 (9)
U2–OH14	2.467 (8)	2.458 (4)	2.484 (10)	2.469 (10)	2.473 (6)	2.452 (11)
U2–OH10	2.615 (8)	2.691 (4)	2.685 (8)	2.609 (10)	2.605 (5)	2.578 (10)
U3–O2	1.741 (11)	1.778 (6)	1.713 (13)	1.693 (15)	1.782 (8)	1.820 (11)
U3–O5	1.793 (10)	1.779 (6)	1.761 (10)	1.805 (11)	1.806 (7)	1.773 (11)
U3–O9	2.236 (8)	2.224 (4)	2.211 (8)	2.225 (10)	2.235 (6)	2.246 (11)
U3–OH15	2.308 (8)	2.290 (4)	2.300 (10)	2.313 (11)	2.325 (6)	2.315 (10)
U3–OH12	2.411 (7)	2.426 (4)	2.404 (9)	2.420 (9)	2.430 (5)	2.433 (11)
U3–OH13	2.461 (8)	2.426 (4)	2.404 (9)	2.461 (9)	2.448 (5)	2.475 (10)
U3–OH14	2.626 (8)	2.441 (4)	2.552 (9)	2.603 (10)	2.605 (6)	2.636 (10)
U4–O8	1.774 (11)	1.789 (5)	1.738 (12)	1.709 (17)	1.793 (8)	1.810 (11)
U4–O6	1.796 (10)	1.781 (6)	1.768 (11)	1.767 (14)	1.781 (8)	1.784 (11)
U4–O9	2.222 (8)	2.249 (4)	2.222 (8)	2.227 (10)	2.223 (6)	2.207 (10)
U4–O11	2.309 (9)	2.246 (4)	2.230 (9)	2.249 (11)	2.304 (6)	2.403 (9)
U4–OH10	2.399 (8)	2.393 (4)	2.395 (9)	2.384 (10)	2.415 (6)	2.378 (10)
U4–OH12	2.479 (8)	2.465 (4)	2.475 (9)	2.464 (9)	2.489 (5)	2.481 (11)
U4–OH13	2.574 (8)	2.591 (4)	2.593 (9)	2.584 (10)	2.566 (6)	2.565 (11)
O11–U4	2.309 (9)	2.246 (4)	2.230 (9)	2.249 (11)	2.304 (6)	2.409(9)
O11–U1	2.302 (9)	2.219 (4)	2.238 (9)	2.281 (12)	2.323 (6)	2.416(10)
O11–U2	2.325 (9)	2.253 (4)	2.242 (9)	2.323 (12)	2.344 (6)	2.434(10)

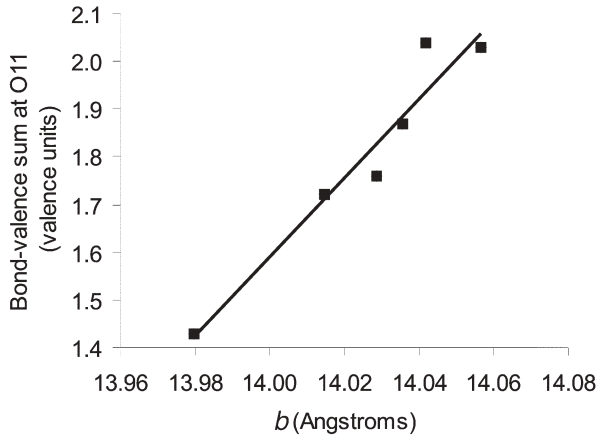

FIGURE 5. The relationship between the bond-valence sum incident at the O11 site in Na-MS and the *b* unit-cell dimension.

Np^{5+} was associated with powders of synthetic uranophane and the Na analog of compreignacite, and that incorporation into the powders was in proportion to the concentration of Np in the mother solution. Burns et al. (2004) found that Np^{5+} was associated with powders of minerals that have sheets of uranyl polyhedra with charges, and interlayer cations, but that Np^{5+} was not incorporated into powders of the two structures considered that contain electroneutral sheets of uranyl polyhedra. On this basis, Burns et al. (2004) proposed that the interlayer cations could be involved in the charge-balance mechanism that permitted substitution of Np^{5+} for U^{6+}.

The sheets of uranyl polyhedra in Na-MS have a residual charge, and the interlayers contain Na. The existence of Na-MS implies that Na can substitute in the interlayer of metaschoepite, which could provide a charge-balance mechanism for substitution of Np^{5+} for U^{6+} within the sheets of uranyl polyhedra. The chemical analysis of crystals of Na-MS-CRY-Np provide compelling evidence that Np is present in the crystal that was synthesized from a solution that was spiked with Np^{5+} (Fig. 3). No suitable Np standard was available for the ICP-MS study, so it was not possible to quantify the Np concentration in the crystals that were analyzed. Using simply the ratio of the count rates for the 237 (Np) and 238 (U) masses, and the known concentration of U in the crystals, it is possible to estimate that the crystals of Na-MS-CRY-Np contain ~500 ppm Np, which is similar to the concentration in the parent solution.

Incorporation of Np into a single crystal of Na-MS-CRY-Np supports the observation of Burns et al. (2004) that Np^{5+} is incorporated into uranyl phases with charged sheets and interlayers. It is especially notable that Burns et al. (2004) did not find Np incorporated into synthetic metaschoepite that was grown in the absence of Na.

DISCUSSION

The close structural and chemical relationship of Na-MS to metaschoepite suggests that Na-MS could occur as a mineral. Indeed, the structure determination for a crystal of natural metaschoepite shows that it is intermediate between end-member metaschoepite, as defined by the synthetic crystal studied by

Weller et al. (2000), and end-member Na-MS, which is approximated by Na-MS-CRY. Given that the X-ray powder diffraction patterns of the two phases are essentially indistinguishable, and that only a detailed chemical analysis would reveal the presence of Na, natural occurrences of Na-MS may have been misidentified as metaschoepite. In a recent study of the thermochemistry of uranyl oxide hydrates, Kubatko et al. (2006) presented the unexpected result that metaschoepite is likely metastable relative to the oxides under geologically relevant conditions. The degree to which Na substitution in the interlayer of metaschoepite may stabilize the structure is unknown, but this effect could be substantial.

Several synthetic Na uranyl oxide hydrates have been reported, but the structures are only known for three. The Na analog of compreignacite appears, on the basis of the similarity of their powder diffraction patterns, to be isostructural with compreignacite (Burns 1998). This structure contains sheets of uranyl pentagonal bipyramids that are based upon the protasite (α-U_3O_8) anion-topology, and Na atoms and H_2O groups are located within the interlayer region. The structure of $Na_2[(UO_2)_3O_3(OH)_2]$ also contains sheets of uranyl pentagonal bipyramids based upon the protasite anion topology, but in this case only Na exists in the interlayer of the structure (Li and Burns 2001). The compound $Na[(UO_2)_4O_2(OH)_5](H_2O)_2$ contains an unusual sheet of uranyl pentagonal bipyramids and distorted uranyl square bipyramids, and Na atoms and H_2O groups are located in the interlayer (Burns and Deely 2002). Na-MS is only the fourth structure known that is based upon sheets of uranyl pentagonal bipyramids with the fourmarierite anion-topology. It possesses a novel sheet composition, and is the first of this structural group that contains Na.

Acknowledgments

The authors thank Lynda Soderholm at Argonne National Laboratory for providing access to radiation laboratories. We thank Schindler of the University of Manitoba for the XPS spectra. This work was initiated with support by the U.S. DOE Environmental Management Science Program under grant DE-FG07-97ER14820, with continuing support from Office of Science and Technology and International (OSTI) of the Office of Civilian Radioactive Waste Management (DE-FC28-04RW12255). The views, opinions, findings, and conclusions or recommendations of the authors expressed herein do not necessarily state or reflect those of the DOE/OCRWM/OSTI.

References cited

Burns, P.C. (1998) The structure of compreignacite, $K_2[(UO_2)_3O_2(OH)_3]_2(H_2O)_7$. Canadian Mineralogist, 36, 1061–1067.

——— (2005) U^{6+} minerals and inorganic compounds: Insights into an expanded structural hierarchy of crystal structures. Canadian Mineralogist, 43, 1839–1894.

Burns, P.C. and Deely, K.M. (2002) A topologically novel sheet of uranyl pentagonal bipyramids in the structure of $Na[(UO_2)_4O_2(OH)_5](H_2O)_2$. Canadian Mineralogist, 40, 1579–1586.

Burns, P.C. and Klingensmith, A.L. (2006) Uranium mineralogy and its impact on neptunium mobility under oxidizing conditions. Elements, 2, 351–356.

Burns, P.C., Miller, M.L., and Ewing, R.C. (1996) U^{6+} minerals and inorganic phases: a comparison and hierarchy of structures. Canadian Mineralogist, 34, 845–880.

Burns, P.C., Ewing, R.C., and Miller, M.L. (1997a) Incorporation mechanisms of actinide elements into the structures of U^{6+} phases formed during the oxidation of spent nuclear fuel. Journal of Nuclear Materials, 245, 1–9.

Burns, P.C., Ewing, R.C., and Hawthorne, F.C. (1997b) The crystal chemistry of hexavalent uranium: Polyhedral geometries, bond-valence parameters, and polymerization of polyhedra. Canadian Mineralogist, 35, 1551–1570.

Burns, P.C., Deely, K.M., and Skanthakumar, S. (2004) Neptunium incorporation into uranyl compounds that form as alteration products of spent nuclear fuel: Implications for geologic repository performance. Radiochimica Acta, 92, 151–159.

Christ, C.L. and Clark, J.R. (1960) X-ray crystallography and crystal chemistry of gowerite. American Mineralogist, 45, 230–235.

Finch, R.J. and Ewing, R.C. (1992) The corrosion of uraninite under oxidizing conditions. Journal of Nuclear Materials, 190, 133–156.

Finch, R.J., Cooper, M.A., Hawthorne, F.C., and Ewing, R.C. (1996) The crystal structure of schoepite, $[(UO_2)_8O_2(OH)_{12}](H_2O)_{12}$. Canadian Mineralogist, 34, 1071–1088.

Finch, R.J., Hawthorne, F.C., and Ewing, R.C. (1998) Structural relations among schoepite, metaschoepite and "dehydrated schoepite." Canadian Mineralogist, 36, 831–845.

Finch, R.J., Buck, E.C., Finn, P.A., and Bates, J.K. (1999) Oxidative corrosion of spent UO_2 fuel in vapor and dripping groundwater at 90 °C. In D.J. Wronkiewicz and J.H. Lee, Eds., Scientific Basis for Nuclear Waste Management XXII. Materials Research Society Symposium Proceedings, 556, 431–438.

Finn, P.A., Hoh, J.C., Wolf, S.F., Slater, S.A., and Bates, J.K. (1996) The release of uranium, plutonium, cesium, strontium, technetium and iodine from spent fuel under unsaturated conditions. Radiochimica acta, 74, 65–71.

Frondel, C. (1958) Systematic mineralogy of uranium and thorium. U.S. Geological Survey Bulletin, 1064.

Kubatko, K.-A., Helean, K.B., Navrotsky, A., and Burns, P.C. (2006) Thermodynamics of uranyl minerals: Enthalpies of formation of uranyl oxide hydrates. American Mineralogist, 91, 685–666.

Li, Y. and Burns, P.C. (2001) The structures of two sodium uranyl compounds relevant to nuclear waste disposal. Journal of Nuclear Materials, 299, 219–226.

Piret, P. (1985) Structure cristalline de la fourmariérite, $Pb(UO_2)_4O_3(OH)_4.4H_2O$. Bull. Minéral., 108, 659–665.

Schindler, M. and Hawthorne, F.C. (2004) A bond-valence approach to the uranyl-oxide hydroxy-hydrate minerals. Canadian Mineralogist, 42, 1601–1628.

Schindler, M., Mutter, A., Hawthorne, F.C., and Putnis, A. (2004a) Prediction of crystal morphology of complex uranyl-sheet minerals. I. Theory. Canadian Mineralogist, 42, 1629–1650.

——— (2004b) Prediction of crystal morphology of complex uranyl-sheet minerals. I. Observations. Canadian Mineralogist, 42, 1651–1666.

Schoep, A. and Stradiot, S. (1947) Crystals of paraschoepite. American Mineralogist, 32, 513–517

Skanthakumar, S., Gorman-Lewis, D., Locock, A., Chiang, M.-H., Jensen, M.P., Burns, P.C., Fein, J., Jonah, C.D., Attenkofer, K., and Soderholm, L. (2004) Changing Np redox speciation in the synchrotron beam. Material Research. Society Proceedings, 802, 151–156.

Weller, M.T., Light, M.E., and Gelbrich, T. (2000) Structure of uranium(VI) oxide dihydrate, $UO_3{\cdot}2H_2O$; synthetic meta-schoeptite $(UO_2)_4O(OH)_6{\cdot}5H_2O$. Acta Crystallographica, B56, 577–583.

Wronkiewicz, D.J., Bates, J.K., Gerding, T.J., Veleckis, E., and Tani, B.S. (1992) Uranium release and secondary phase formation during unsaturated testing of UO_2 at 90 °C. Journal of Nuclear Materials, 190, 107–127.

Wronkiewicz, D.J., Bates, J.K., Wolf, S.F., and Buck, E.C. (1996) Ten-year results from unsaturated drip tests with UO_2 at 90 °C: implications for the corrosion of spent nuclear fuel. Journal of Nuclear Materials, 238, 78–95.

Manuscript received June 19, 2006
Manuscript accepted November 16, 2006
Manuscript handled by Sergey Krivovichev